PALEOCEANOGRAPHY, VOL. 12, NO. 2, PAGES 175-190, APRIL 1997

Comparison of Imbrie-Kipp transfer function and modern analog temperature estimates using sediment trap and core top foraminiferal faunas

J. D. Ortiz[1] and A. C. Mix

College of Oceanic and Atmospheric Sciences, Oregon State University, Corvallis

Abstract. We evaluate the reliability of statistical estimates of sea surface temperature (SST) derived from planktonic foraminiferal faunas using the modern analog method and the Imbrie-Kipp method. Global core top faunas provide a calibration data set, while modern sediment trap faunas are used for validation. Linear regression of core top predicted SST against atlas SST generated slopes close to one for both methods. However, the Imbrie-Kipp transfer function temperature estimates had an intercept 1.3°C warmer than modern analog estimates and 1.7°C warmer than recorded atlas SST. The RMS error for the core top data set using the modern analog method (1.5°C) was smaller than that of the Imbrie-Kipp method (1.9°C). SST errors for the sediment trap faunas were not statistically different from those of the core top data set, regardless of method. Developing Imbrie-Kipp transfer functions for limited regions reduced the RMS variability but introduced residual structure not present in the global Imbrie-Kipp transfer function. Dissolution simulations with the sediment trap sample which generated the warmest SST residual for both methods suggests that the loss of delicate warm water foraminifera from midlatitude sediments may be the cause of this thermal error. We conclude that (1) the faunal structure of sediment trap and core top assemblages are similar; (2) both methods estimate SST reliably for modern foraminiferal flux assemblages, but the modern analog method exhibits less bias; and (3) both methods are relatively robust to samples with low communality but sensitive to selective faunal dissolution.

Introduction

Because sea surface temperature (SST) provides an important climate diagnostic on a variety of spatial and temporal scales, we assess the reliability of paleotemperature reconstructions derived from planktonic foraminiferal faunas. The two techniques most commonly used to estimate paleotemperature from these microfossils are the transfer function method of *Imbrie and Kipp* [1971] and the modern analog method of *Hutson* [1980] as modified by *Prell* [1985]. Do these two methods provide consistent, unbiased paleotemperature estimates?

A potential problem is most evident in the temperature dilemma of the low-latitude last glacial maximum (LGM) ocean where microfossil paleotemperature reconstructions differ from other methods by as much as 2°-3°C and are inconsistent with some climate model results [*Rind and Peteet*, 1985]. Statistical reconstructions based on microfossils [e.g., *CLIMAP*, 1976, 1981] suggest that low - latitude SST was at most 2°-3°C cooler than modern. This 2°-3°C cooling was indicated by several types of microfossils [*Molfino* et al. 1982].

Broecker [1986] compared these findings with planktonic foraminiferal $\delta^{18}O$ and concluded the $\delta^{18}O$ data was also reasonably consistent with a 2°-3°C cooling. *Stott and Tang* [1996] reached a similar conclusion in their study of tropical $\delta^{18}O$ measurements. The recent study of *Broccoli and Marciniak* [1996] suggests that point by point comparisons of climate model output and observations reduces some of the low-latitude SST discrepancy. Unfortunately, they could not make a clear determination as to the validity of one approach over the other.

In contrast, results derived from coral Sr/Ca paleothermometry [e.g., *Beck* et al. 1992; *Guilderson* et al. 1994] and a variety of terrestrial based methods [e.g., *Rind and Peteet*, 1985] suggest that low-latitude glacial SST may have been as much as 5°-6°C cooler than modern. Because of this apparent discrepancy, we reevaluate the reliability of statistically based microfossil SST estimates derived from planktonic foraminiferal faunas using the transfer function method of *Imbrie and Kipp* [1971] and the modern analog method of *Hutson* [1980] as modified by *Prell* [1985]. Our analysis differs from previous sediment based studies in that we estimate SST for sediment trap assemblages caught in the water column as well as for core tops. This test is designed to assess whether smoothing and modification involved with the generation of the fossil record induces bias in foraminiferal faunal SST estimates.

[1]Now at Lamont-Doherty Earth Observatory of Columbia University, Palisades, New York.

Paper number 96PA02878.
0883-8305/97/96PA-02878$12.00

Methods

Core Top and Sediment Trap Data Sets

Prell [1985] tested the modern analog method of *Hutson* [1980] and demonstrated that with slight modification, it yields essentially identical SST results to the transfer function approach of *Imbrie and Kipp* [1971]. These tests were conducted using core top foraminiferal faunas from the three major ocean basins. Unfortunately, validation of paleotemperature proxy methods based on core top data alone has several potential sources of bias. These include (1) stratigraphic sampling errors, (2) dissolution errors, (3) bioturbation which mixes together foraminiferal shells from different times, and (4) the possibility that the statistical correlation to SST observed in the core top faunas is not present in the living faunas but rather is a secondary artifact, caused, for example, by the correlation of SST with other environmental variables.

The first three problems may be expressed as either random or systematic errors in the SST estimates derived from either method. We assess random error by calculating the RMS error for each method. We assess systematic bias in each method by determining the slope and intercept of actual versus estimated SST regressions and by testing residuals for statistically significant trends. To address the fourth problem, we assembled a validation data set of foraminiferal faunas from 13 sediment trap locations (Figure 1) including our three sites at 42°N in the California Current and a previously unpublished data set from a site in the equatorial Pacific, Manganese Nodule Project (MANOP) Site C.

We compare the sediment trap validation data set with a calibration data set of 1121 core tops (Figure 2) composed of those from *Prell* [1985] and selected samples from *Parker and Berger* [1971], *Coulbourn* et al. [1980], and *Thompson* [1981]. Samples in these data sets were screened to exclude duplicates and samples with erroneous locations (A. E. Morey and A. C. Mix, personal communication, 1996). To account for differences in the taxonomy used by various workers, we employed a subset of 27 taxonomic species and lumped some taxonomically similar species into morphologic groups. The four morphologic groups we employed are (1) *G. ruber* (total), which includes both the pink and white varieties; (2) *G. sacculifer* (total), which includes *G. trilobus* and *G. sacculifer*; (3) *G. menardii* (total), which includes *G. menardii*, *G. menardii flexuosa* (=*neoflexuosa*), and *G. tumida*; and (4) *N. dutertrei* (which includes the "*Neogloboquadrina pachyderma* - *Neogloboquadrina dutertrei* (*P-D*) intergrade" category of *Kipp* [1976]). We believe the *P-D* intergrade category to be conspecific with *N. dutertrei* based on our plankton tow and sediment trap studies [*Ortiz and Mix*, 1992; *Ortiz* et al. 1995].

The sediment trap data are of known modern age and essentially free of dissolution. Table 1 provides information regarding the locations of the sediment trap faunas and their sources, while Table 2 lists the flux-weighted foraminiferal faunas from these locations. The sediment trap samples have the disadvantage of short integration times, ranging from several months to 6 years. Poorly resolved interannual variation may affect the results. To assess this effect, the modern analog method and Q-mode factor analysis provide quantitative estimates of how different the sediment trap faunas are from the sedimentary faunas.

Unlike the core top data set, the sediment trap faunal counts are not all based on the >150 μm size fraction. Ideally, the sediment trap samples should be processed in a manner which is

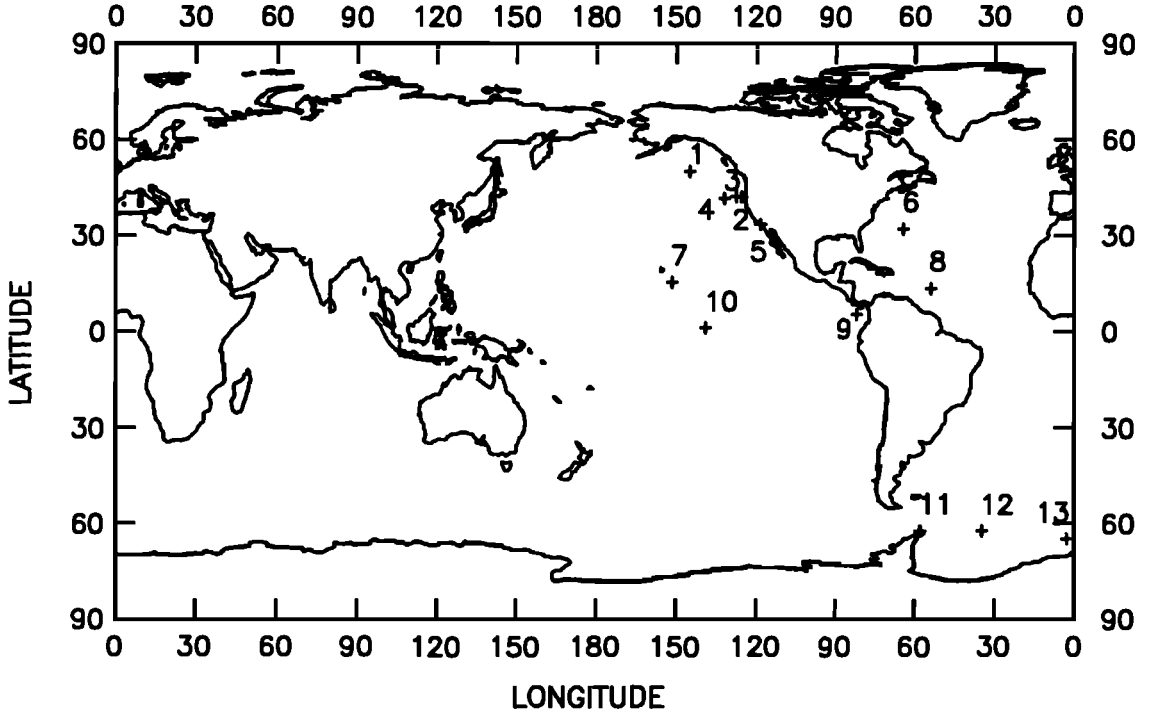

Figure 1. Locations of the 13 sediment trap faunas used in the paper. Numbers next to each trap location correspond to map indices in Table 1. References for each published sample are listed in Table 1.

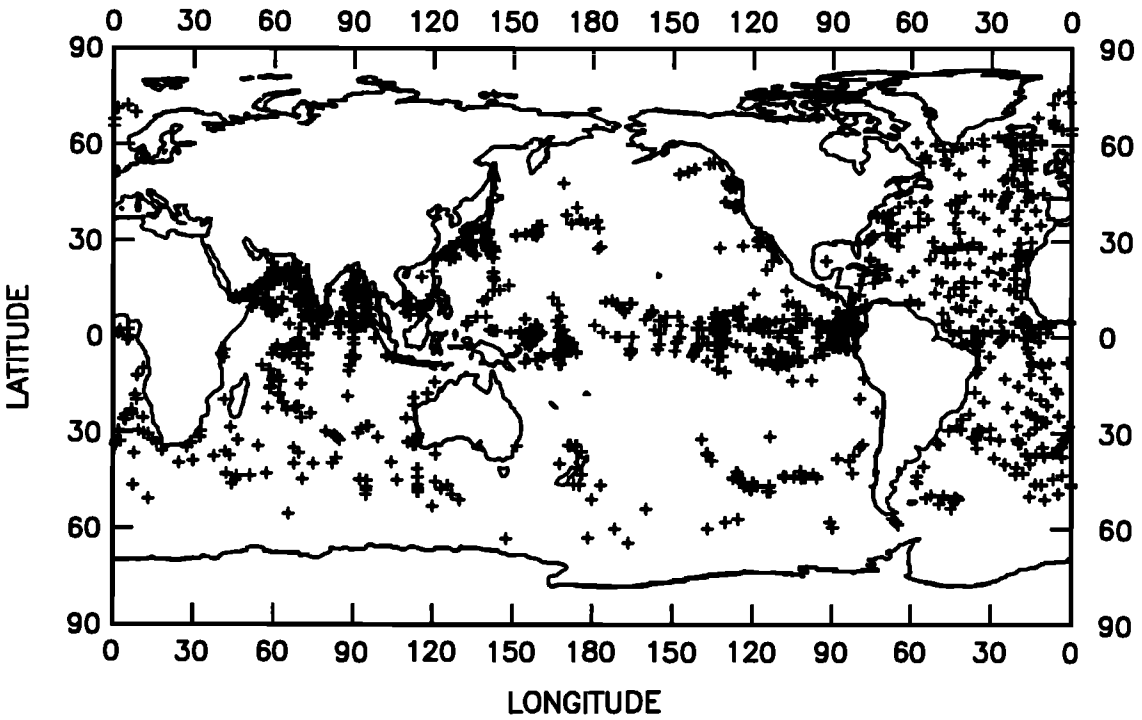

Figure 2. Locations for the 1121 core top samples in the global core top data set.

identical to that of the core top sediments. In our studies we have measured both the 125-150 and >150 μm size fractions. This allows us to easily compare our samples to >150 μm sediments or >125 μm sediment trap samples. We recommend that future sediment trap and plankton tow studies follow this procedure or focus on the >150 μm size fraction. While variations in sieve size introduce some uncertainty in the sediment trap to core top comparison, the residual errors we obtained are not correlated with sieve size variations. Any bias introduced by this source of error is thus not systematic. These potential sources of error will be evaluated further in the discussion to follow.

Q-Mode Factor Analysis and Imbrie-Kipp Transfer Functions

As a first step in the comparison of core top and sediment trap faunas, we calculated a Q-mode factor model for the global core top database following *Imbrie and Kipp* [1971]. Q-mode factor analysis provides an objective, quantitative means of simplifying complex data sets. This is accomplished by decomposing the core top data matrix ($\mathbf{U}_{ct}$) into a factor score matrix ($\mathbf{F}_{ct}$), a factor loading matrix ($\mathbf{B}_{ct}$), and an error matrix ($\mathbf{E}_{ct}$):

$$\mathbf{U}_{ct} = \mathbf{B}_{ct}\,\mathbf{F}_{ct} + \mathbf{E}_{ct} \quad (1)$$

$\mathbf{U}_{ct}$, the core top percent abundance data, is based on counts of n=27 planktonic foraminiferal taxa in N=1121 coretops. Each core top fauna in $\mathbf{U}_{ct}$ is row normalized so that its sum of squares is unity. The elements of the factor score matrix, $\mathbf{F}_{ct}$, describe m varimax rotated assemblages composed of weighted contributions from each of the 27 taxa (see Table 3). A varimax rotation is applied to $\mathbf{F}_{ct}$ so that the resulting assemblages remain close to the centroid of the sample data. This rotation has the advantage of producing orthogonal assemblages with generally positive coefficients that are more easily interpreted than an unrotated solution. The elements of $\mathbf{B}_{ct}$ describe the relative contribution of each varimax assemblage to each core top sample. The model fit is described by its communality (the sum of squares of $\mathbf{B}_{ct}$ or the normalized vector length), which is a linear measure of the fraction of information retained from each sample [*Imbrie and Kipp*, 1971]. A perfect model fit is achieved when communality goes to 1, and $\mathbf{E}_{ct}$=0.

We use the transpose of the core top factor score matrix ($\mathbf{F}^{T}_{ct}$) to evaluate the structure of the sediment trap data matrix ($\mathbf{U}_{st}$) by determining a factor loading matrix ($\mathbf{B}_{st}$) for the sediment trap data set:

$$\mathbf{U}_{st}\,\mathbf{F}^{T}_{ct} = \mathbf{B}_{st} + \mathbf{E}_{st} \quad (2)$$

This assumes that the structure of the core top assemblages apply to the sediment trap faunas. If this assumption is not correct, the resulting sample communality will be low, and the elements of $\mathbf{E}_{st}$ will be nonzero. If the distribution of the core top assemblages are controlled by their environment, then $\mathbf{B}_{st}$ should produce distinct patterns when plotted against a controlling environmental variable such as SST [*Imbrie and Kipp*, 1971]. However, if the fundamental structure of the sediment trap faunas differs from that of the core top faunas, then the distribution pattern of $\mathbf{B}_{st}$ with respect to SST will not match that of $\mathbf{B}_{ct}$.

The core top factor loadings in $\mathbf{B}_{ct}$ were regressed against SST to develop a stepwise least squares transfer function.

Table 1. Locations and Sources of the Sediment Trap Faunas

Map Index and Trap Location	Latitude, °N	Longitude, °W	Trap Depth, m	Duration, months	Sieve Size, μm	Seasons	Reference
1, Gulf of Alaska	50.00	-145.00	3800	52.0	>125	annual	*Sautter and Thunell* [1989]
2, Nearshore	42.09	-125.77	1000	12.0	>150	annual	*Ortiz and Mix* [1992]
3, Midway	42.19	-125.58	1000	12.0	>150	annual	*Ortiz and Mix* [1992]
4, Gyre	41.54	-132.02	1000	12.0	>150	annual	*Ortiz and Mix* [1992]
5, San Pedro Basin	33.55	-118.50	500	7.0	>125	Jan.-July	*Sautter and Thunell* [1991]
6, Sargasso Sea	32.08	-64.25	3200	72.0	>125	annual	*Deuser* [1987]; *Deuser and Ross* [1989]
7, Central Pacific	15.35	-151.47	978	2.0	>100	Sept.-Oct.	*Thunell and Honjo* [1981]
8, Tropical Atlantic	13.52	-54.00	389	3.2	>100	Dec.-Feb	*Thunell and Honjo* [1981]
9, Panama Basin	5.35	-81.88	890	12.0	>125	annual	*Thunell and Reynolds* [1984]
10, MANOP Site C	1.00	-139.00	1089	29.5	>150	annual	this study
11, King George B	-62.37	-57.83	687	5.4	>125	Nov.-May	*Donner and Wefer* [1994]
12, North Weddell Sea	-62.44	-34.76	868	13.8	>125	annual	*Donner and Wefer* [1994]
13, Maud Rise	-64.91	-2.55	4456[a]	37.3	>125	annual	*Donner and Wefer* [1994]

[a] Averaged from three depths.

Following *Imbrie and Kipp* [1971], we include squared and cross product terms for each factor in the stepwise regression. These terms are included in the final regression if their partial F value exceeds the critical 5% significance threshold. Squared and cross product terms are included so that our results can be compared with equations of the type developed for *CLIMAP* [1976, 1981] and because each factor may exhibit nonlinear, parabolic responses to temperature and/or interactive effects [*Imbrie and Kipp*, 1971]. The regression coefficients from the global Imbrie-Kipp transfer function are used with the sediment trap factor loadings in $\mathbf{B}_{st}$ to determine Imbrie-Kipp temperature estimates for each of the sediment trap faunas.

The transfer function SST is compared with seasonally weighted SST from each trap location obtained from *Levitus* [1982]. The SST weighting for each trap temperature is determined from its duration and deployment season. This procedure is necessary because some of the sediment trap deployments did not sample the entire annual cycle. Assigning an annual average temperature to a subannual foraminiferal fauna would introduce an unrealistic temperature bias to our comparisons.

The Modern Analog Method

We calculate modern analog SST from the sediment trap faunas using the core tops as the calibration data set. We then compare these SST estimates with measured SST values from *Levitus* [1982] at the sediment trap locations. As a final test of the modern analog method, we estimated modern analog SST for each core top in the database by comparison against every other core top in the database. This global calculation is similar to the separate ocean basin calculations of *Prell* [1985]. It allows us to evaluate the level of variation in the sediment trap versus core top comparison against the level of variation observed in the core top data set.

The modern analog method compares planktonic foraminiferal assemblages in samples with unknown environmental conditions (SST in this application) with core tops from locations with known environmental conditions. The two basic assumptions for the modern analog method are similar to those of the Imbrie-Kipp transfer function. The first assumption is that similar foraminiferal faunal assemblages are produced by similar suites of environmental conditions. The second assumption is that SST is the environmental variable which determines variation in foraminiferal assemblages or is correlated with environmental variables which determine foraminiferal variation.

The first assumption holds well for most of the world ocean. One notable exception to the rule occurs at very high northern and southern latitudes. At these climatic extremes, the foraminiferal fauna becomes essentially monospecific, dominated by left-coiling *N. pachyderma*. However, high southern latitudes are cooler by 1°-2°C than high northern latitudes. Because foraminiferal faunas attain essentially monospecific status well before extremely cold southern ocean SST values are reached, use of a global data set to predict modern analog SST at extremely high latitudes can give erroneous results due to the averaging of SST from both hemispheres. To avoid this problem, we follow the standard

Table 2. Flux-Weighted Percent Abundance for the Sediment Trap Foraminiferal Faunas as Numbered in Table 1

Taxon[a]	Map Locations												
	1	2	3	4	5	6	7	8	9	10	11	12	13
O. universa	2.9	1.8	8.6	37.0	4.9	1.1	2.7	0.3	0.4	0.2	0.0	0.0	0.0
G. conglobatus	0.0	0.0	0.0	0.0	0.0	0.3	2.0	0.8	0.3	0.6	0.0	0.0	0.0
G. ruber (total)[b]	0.0	1.8	4.8	13.0	2.5	33.4	14.8	38.4	14.9	21.6	0.0	0.0	0.0
G. tenelus	0.0	0.0	0.0	0.0	0.0	0.0	17.3	0.0	0.1	1.0	0.0	0.0	0.0
G. sacculifer (total)[b]	0.0	0.0	0.0	0.0	0.0	0.4	5.2	10.0	2.9	9.6	0.0	0.0	0.0
S. dehiscens	0.0	0.0	0.0	0.0	0.0	0.0	0.0	0.3	0.0	0.0	0.0	0.0	0.0
G. aequilateralis	0.0	0.0	0.0	0.0	1.4	4.6	0.4	5.6	1.4	4.5	0.0	0.0	0.0
G. calida	0.0	1.8	0.0	6.0	0.0	0.0	0.9	0.5	0.6	6.2	0.0	0.0	0.0
G. bulloides	2.9	9.7	15.2	13.0	35.4	32.2	0.9	0.3	13.3	8.2	0.0	0.0	0.0
G. faclonensis	0.0	20.4	4.8	6.0	0.0	0.0	0.0	0.0	0.0	1.4	0.0	0.0	0.0
G. digitata	0.0	0.0	0.0	0.0	0.3	0.0	0.4	0.0	0.1	0.0	0.0	0.0	0.0
G. rubescens	0.0	0.0	0.0	0.0	0.0	1.1	23.3	1.5	0.3	2.5	0.0	0.0	0.0
G. quinqueloba	58.2	1.8	6.7	3.0	24.1	0.0	0.2	0.8	1.9	0.0	0.0	0.0	6.3
Left-coiling *N. pachyderma*	16.8	27.4	6.7	0.0	0.2	0.0	0.0	0.0	0.0	0.0	90.0	96.0	92.0
Right-coiling *N. pachyderma*	11.8	14.2	21.9	7.0	17.5	0.0	0.0	0.0	3.0	0.2	10.0	4.0	1.7
N. dutertrei	0.0	17.6	16.2	2.0	4.9	0.9	0.2	5.6	27.2	9.4	0.0	0.0	0.0
G. conglomerata	0.0	0.0	0.0	0.0	0.0	0.0	0.9	0.0	0.3	2.0	0.0	0.0	0.0
G. hexagona	0.0	0.0	0.0	0.0	1.4	0.0	4.3	0.0	1.3	2.0	0.0	0.0	0.0
P. obliquiloculata	0.0	0.0	0.0	0.0	0.0	0.7	0.0	0.0	0.3	8.2	0.0	0.0	0.0
G. inflata	0.0	0.0	0.0	0.0	0.0	1.2	0.0	0.0	0.0	0.0	0.0	0.0	0.0
Left-coiling *G. truncatulinoides*	0.0	0.0	0.0	0.0	0.0	9.3	0.0	0.0	0.0	0.0	0.0	0.0	0.0
Right-coiling *G. truncatulinoides*	0.0	0.0	0.0	0.0	0.0	0.0	0.0	0.0	0.0	0.0	0.0	0.0	0.0
G. crassaformis	0.0	0.0	0.0	0.0	0.0	0.2	0.0	0.0	0.0	0.0	0.0	0.0	0.0
G. hirsuta	0.0	0.0	0.0	0.0	0.0	3.9	0.0	0.0	0.0	0.0	0.0	0.0	0.0
G. scitula	0.2	1.8	8.6	3.0	0.0	0.0	2.5	6.4	0.2	1.5	0.0	0.0	0.0
G. menardii (total)[b]	0.0	0.0	0.0	0.0	0.0	0.0	0.4	3.6	4.7	2.3	0.0	0.0	0.0
G. glutinata	7.2	1.8	6.7	7.0	5.2	10.8	17.0	23.5	23.5	6.5	0.0	0.0	0.0

[a]Some rare species that were reported in the original sources are omitted here from the flux weighted percents because these taxa were not uniformly reported by all workers. These catagories were essentialy treated as unidentified.

[b]*G. ruber* (total) = *G. ruber* (white) and *G. ruber* (pink); *G. sacculifer* (total) = *G. sacculifer* and *G. trilobus*; *G. menardii* (total) = *G. menardii*, *G. tumida*, and *G. menardii neoflexuosa*.

Table 3. Factor Scores for the Seven-Factor, Varimax Rotated,Q-Mode Factor Model Based on 1121 Core Tops

Taxon	Factor 1, *G. rub.* T./ *G.sac.* T.	Factor 2, *G. men.* T.	Factor 3, *N. pac.* L.	Factor 4, *G. inf.*	Factor 5, *N. dut.*	Factor 6, *G. bull./ G. glut.*	Factor 7, *P. obliq.*
O. universa	0.02	0.00	0.00	0.03	0.00	0.01	0.01
G. conglobatus	0.05	0.01	-0.00	0.00	-0.00	0.00	0.04
G. ruber (total)[b]	0.90[a]	-0.05	0.01	0.06	-0.05	-0.11	-0.11
G. tenelus	0.04	-0.01	-0.01	-0.00	-0.00	0.02	0.00
G. sacculifer (total)[b]	0.31[a]	0.07	0.03	-0.02	0.04	-0.08	0.02
S. dehiscens	0.00	0.03	0.00	0.00	-0.00	-0.00	0.01
G. aequilateralis	0.10	0.01	-0.01	-0.00	0.01	0.02	0.11
G. calida	0.05	-0.01	-0.01	0.01	0.01	0.01	0.06
G. bulloides	-0.03	0.06	0.17	0.13	-0.06	0.81[a]	-0.16
G. falconensis	0.05	-0.01	-0.04	0.13	-0.03	0.05	-0.02
G. digitata	0.01	0.02	0.00	0.01	-0.00	0.00	-0.00
G. rubescens	0.03	-0.01	-0.01	-0.01	-0.00	0.02	0.01
G. quinqueloba	-0.01	-0.01	0.12	0.01	0.01	0.06	-0.01
Left-coiling *N. pachyderma*	0.02	-0.00	0.97[a]	-0.03	-0.01	-0.07	0.04
Right-coiling *N. pachyderma*	-0.04	-0.09	0.04	0.26	0.10	0.05	0.04
N. dutertrei	0.02	0.03	0.02	0.08	0.98[a]	0.01	0.00
G. conglomerata	0.01	0.04	0.00	-0.01	0.01	0.00	0.03
G. hexagona	0.02	0.01	-0.00	-0.01	0.01	0.02	-0.01
P. obliquiloculata	0.01	0.12	0.03	0.03	-0.04	-0.03	0.93[a]
G. inflata	-0.02	0.03	-0.02	0.92[a]	-0.09	-0.07	0.03
Left-coiling *G. truncatulinoides*	0.02	0.01	-0.01	0.09	-0.02	0.00	-0.03
Right-coiling *G. truncatulinoides*	0.02	0.01	0.01	0.10	-0.03	0.01	-0.02
G. crassaformis	0.01	0.01	0.00	0.02	0.00	-0.01	-0.00
G. hirsuta	0.01	0.00	-0.01	0.05	-0.01	-0.01	-0.01
G. scitula	0.01	-0.00	-0.00	0.03	0.00	0.02	-0.00
G. menardii (total)[b]	0.05	0.97[a]	-0.03	-0.04	-0.01	0.04	-0.07
G. glutinata	0.26	-0.14	-0.12	-0.12	0.05	0.55[a]	0.27
Information per Factor[c]	27.4%	12.1 %	8.4%	12.5%	14.6%	11.5%	5.1%

[a]Dominant species.
[b]*G. ruber* (total) = *G. ruber* (white) and *G. ruber* (pink); *G. sacculifer* (total) = *G. saculifer* and *G. trilobus*; *G. menardii* (Total) = *G. menardii*, *G. tumida*, and *G. menardii neoflexuosa*.
[c]Total information explained: 91.5%.

procedure of *Prell* [1985] and compare high-latitude (northern) southern hemisphere trap samples against (northern) southern hemisphere core top samples only.

Assessment of the second assumption is more problematic. For relatively small spatial scales and short timescales, absolute abundance assemblages of planktonic foraminifera from plankton tow and seasonal sediment traps demonstrate greater control by biological factors (food availability and light) than temperature [*Fairbanks and Wiebe*, 1980; *Watkins* et al. 1996; *Ortiz and Mix*, 1992; *Ortiz* et al. 1995]. Here we focus on the relative abundance of foraminiferal assemblages at large spatial scales, integrated over time scales of generally longer than the annual cycle. Under such conditions, foraminiferal core top assemblages exhibit relatively strong relationships to SST [e.g., *Imbrie and Kipp*, 1971; *Prell*, 1985]. We wish to determine whether the correlation to SST is also present in the global data set of temporally averaged sediment trap faunas.

Temperature estimates based on the modern analog method depend on averages of sample-by-sample comparisons. *Hutson* [1980] used the cosine theta angle as a measure of the multivariate distance (i.e., dissimilarity) between two foraminiferal faunas. Empirical pollen studies suggest that the squared chord distance provides more reliable results than several other dissimilarity measures including the cosine theta angle [*Prentice*, 1980; *Overpeck* et al. 1985]. The use of the squared chord distance tends to increase the importance of rare species and decrease the importance of abundant ones so that differences in the abundant species alone do not dominate the dissimilarity estimate. *Prell* [1985] demonstrated that the squared chord distance worked well with foraminiferal faunas. Accordingly, we use the squared chord distance between the target sample and each core top in the database as a measure of intersample dissimilarity:

$$d_{ij} = \sum_{k=1}^{m} [p_{ik}^{1/2} - p_{jk}^{1/2}]^2 \quad (3)$$

In this notation, d_{ij} is the squared chord distance between the ith and jth samples, while p_{ik} and p_{jk} represent the fractional percentages of the kth species in samples i and j. The 27 taxonomic categories used to calculate the squared chord distance are the same as those used in the Q-mode factor analysis described above (Table 3). Just as the communality provides a quantitative estimate of how well a foraminiferal fauna is explained by a factor model, the average sample dissimilarity provides a quantitative estimate of the similarity between a target fauna and its closest analogs. Empirical studies suggest that values of $d_{ij} < 0.25$ yield reliable analogs (W. Prell, personal communication, 1996). We tested this rule

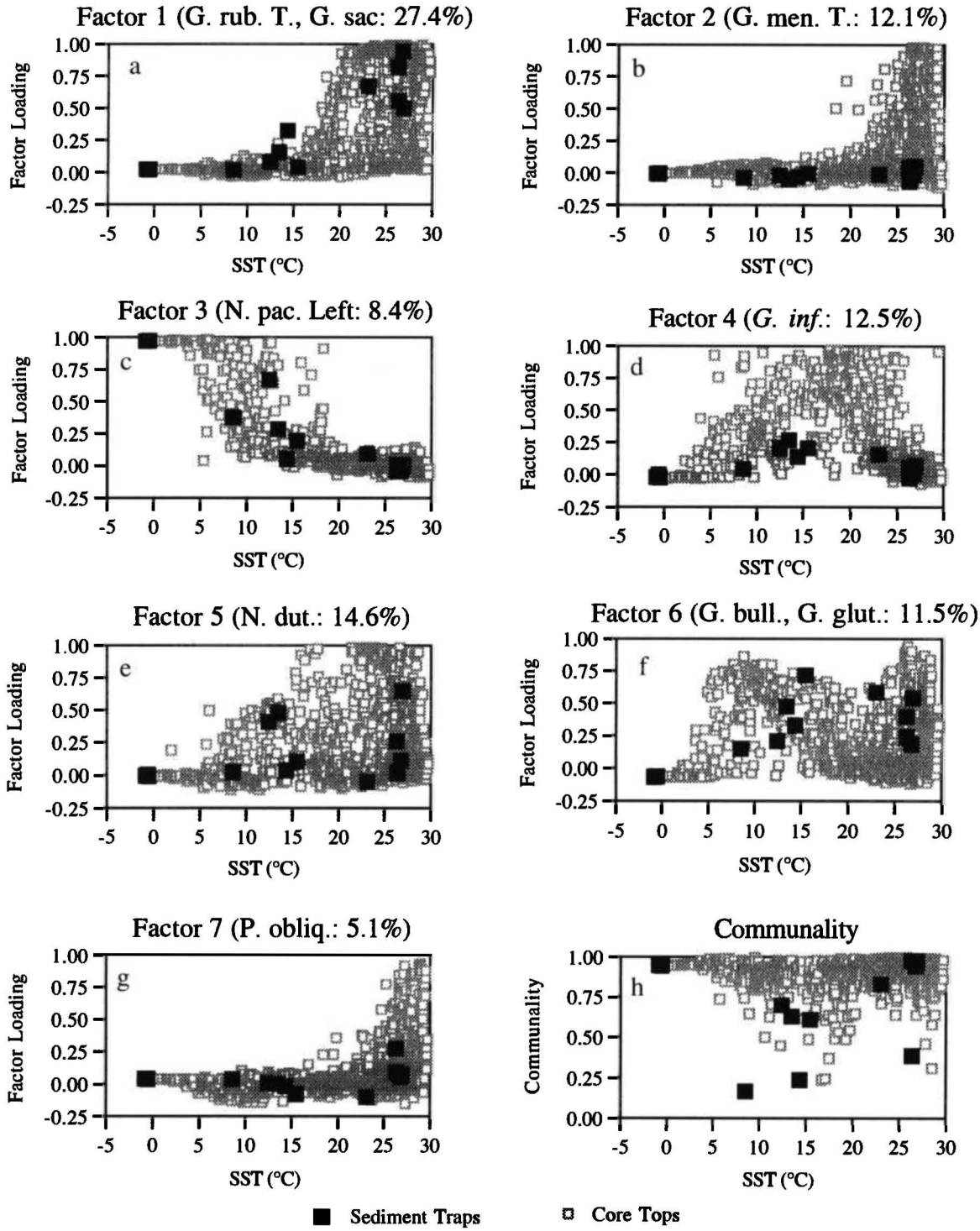

Figure 3. Factor loadings and communalities versus sea surface temperature for the global Q-mode factor model described in the text. Core tops are small open squares, while sediment traps are large solid squares. Abbreviated names list the dominant species for each factor. Figures 3a-3g correspond to factors 1-7. Figure 3h displays sample communalities.

of thumb by calculating d_{ij} for each sample in the core top data set in comparison with all others. While values of d_{ij} are not normal in distribution, natural log transformed values of d_{ij} are approximately log normal. We note that 97% of the faunas in the core top data set have an average d_{ij} value for their top five analogs that is <0.20 and that 99% of the faunas have average d_{ij} values <0.26. W. L. Prell (personal communication, 1996) reports similar experience with applications of this method to foraminiferal faunas. We thus choose 0.20 as a conservative cutoff limit.

Using the values of d_{ij} as the selection criteria, the SST values from the five core tops least dissimilar to the target sample are averaged to estimate the modern analog SST for that sample. We use arithmetic, rather than weighted averages, when calculating analog SST estimates. Tests we have conducted demonstrate that SST averages weighted by the individual dissimilarity estimates as proposed by *Hutson* [1980] are not significantly different from arithmetic averages. We did not experiment with more sophisticated geographic weighting methods [e.g., *Pflaumann* et al. 1996].

Results

Q-Mode Factor Analysis

Seven factor assemblages together account for 91.5% of the information in the global core top data set. The addition of an eighth factor assemblage would have increased the total information explained by only 2.4% to 93.9%. Models with few assemblages generated groupings that were ecologically less distinct. Table 3 lists the factor scores for the seven assemblages we chose to retain. The seven factors group species with similar distributions into assemblages which individually account for 5-27% of the total information. These assemblages correspond roughly to oceanographic environments. For example, factor 1, which is dominated by *G. ruber* and *G. sacculifer*, is important in warm, oligotrophic regions, while factor 3, composed of left-coiling *N. pachyderma*, is indicative of cold, high-latitude extremes.

To compare the sediment trap and core top foraminiferal faunas, we apply the core top factor scores to the sediment trap data and extract factor loadings for each sample. Plots of factor loading against SST from *Levitus* [1982] serve as a useful indication of sample environments (Figure 3). In general, factor loadings from the two data sets have similar trends with respect to SST. This is most clear for factors 1, 3, 5, and 6 (Figure 3).

Potential differences between the two data sets do exist. The amplitude of the factor loadings for factors 2, 4, and 7 are diminished in the sediment trap assemblages relative to the core top assemblages. The dominant species in these factors are relatively rare in the sediment traps and abundant in some of the core top sediments. This could be a sampling problem or may reflect a bias in the sediments. All of the species involved have heavily calcified shells, suggesting that dissolution may enrich them in the sediments relative to their abundance in the overlying water column.

The model communality measures how much of the information content of the foraminiferal faunas is explained by the factor model (Figure 3h). For both core top and sediment trap faunas the factor model explains adequate amounts of sample information at latitudinal extremes (SST <9°C or >20°C) but explains little information in the midlatitude faunas at SST from 9°-15°C. Note, however, that this pattern is seen in the communalities of both the core top and sediment trap faunas, suggesting that a similar process contributes to the effect in both data sets. We explore how low sample communality may affect the SST estimates derived from the Imbrie-Kipp and modern analog methods in the discussion section.

Table 4. Coefficients for the Global Imbrie-Kipp Transfer Function

Term	Coefficient
Intercept	27.6
Factor 3	-46.2
Factor 4	-26.2
Factor 3 squared	21.2
Factor 4 squared	18.6
Factor 5 squared	-1.1
Factor 6 squared	-3.3
Factor 7 squared	3.0
Factor 1 × factor 3	72.8
Factor 1 × factor 4	4.5
Factor 1 × factor 6	5.4
Factor 2 × factor 3	55.9
Factor 2 × factor 4	13.4
Factor 2 × factor 6	9.3
Factor 2 × factor 7	-3.8
Factor 3 × factor 4	21.4
Factor 3 × factor 5	20.0
Factor 3 × factor 6	10.6
Factor 4 × factor 6	-3.1
Factor 4 × factor 7	19.7
Factor 5 × factor 6	-6.0

Global Imbrie-Kipp Transfer Function

A statistically significant SST transfer function was developed using the core top data set. The terms for this global Imbrie-Kipp transfer function are listed in Table 4. This regression, based on 1121 samples, is significant at $p \ll 0.01$, has an r^2 of 0.93, and an RMS error of 1.9°C. The core top SST estimates have a slope of 0.93±0.02 and an intercept of 1.7±0.4 at the 95% confidence limit with respect to *Levitus* [1982] SST (Figure 4a). The slope of the core top regression is significantly different from one (with 95% confidence), given the sample size of 1121 core tops.

To compare the core top and sediment trap assemblages, we applied the core top transfer function to the sediment trap factor loadings (Figure 4, Table 5). When the transfer function is applied to the sediment trap samples, the SST estimates follow a slope of 0.92±0.16 and an intercept of 4.2±2.8 at the 95% confidence limit with respect to the *Levitus* [1982] SST values. The RMS error for the sediment trap SST estimates with this method was 2.6°C. The slope of the sediment trap relationship (0.92±0.16) is not significantly different from that of the core tops, or from one. However, as was the case for the core tops, the 95% confidence interval on the regression intercept indicates a warm bias in the sediment trap SST estimates (Figure 4b). A two-sided *t*-test of the 3.0°C average Imbrie Kipp-SST sediment trap residual demonstrates that this bias is significant at $p \ll 0.01$ (degrees of freedom (*df*) =12, RMSE=2.6°C, *t*-value=4.18 > *t*-crit@0.01=3.055). The sediment trap SST estimates also appear to exhibit a residual trend as a function of the factor model communality. However, it is unlikely that this feature is statistically significant: The trend is not present in the core top SST residuals and occurs only at very low communality in the sediment trap residuals (Figure 4c).

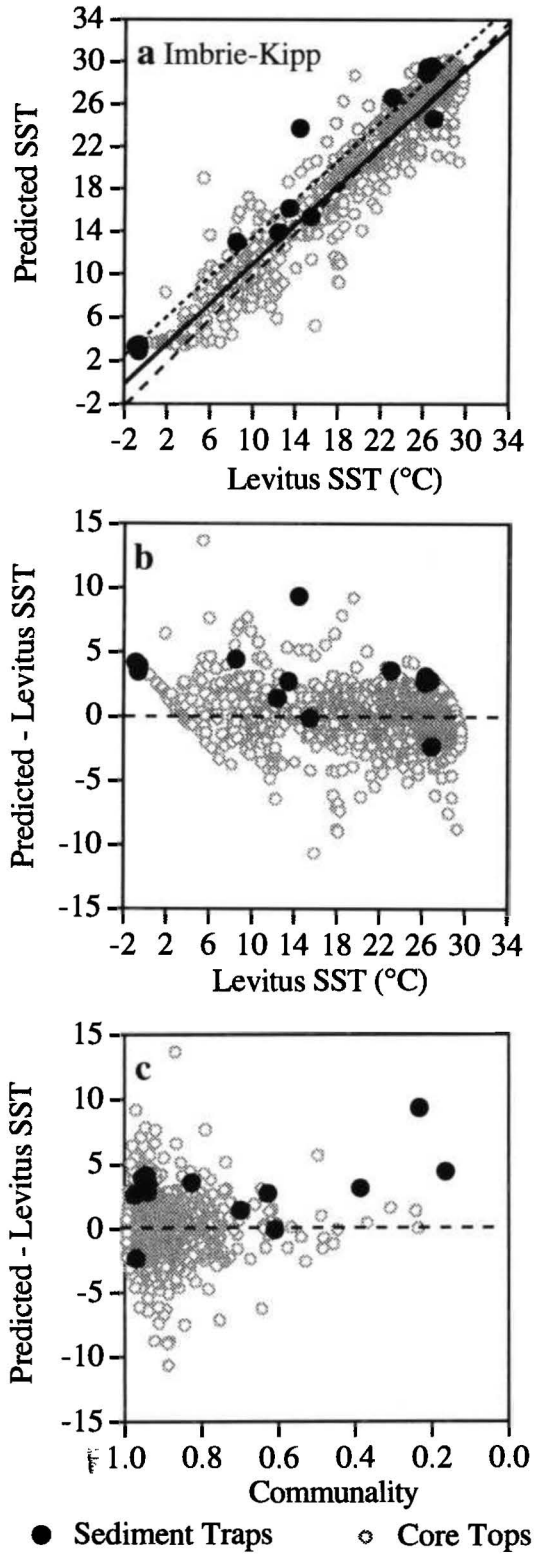

Figure 4. Results of the global Imbrie-Kipp transfer function. (a) *Levitus* [1982] sea surface temperature (SST) versus predicted SST. Diagonal lines mark a 1:1 relationship (long dashed line), and least squares regressions for the core top (solid line) and sediment trap (short dashed line) samples. (b) Levitus SST versus residual SST. (c) Residual SST versus factor model communality. Lower communalities denote weaker factor model fit. Note reversed communality axis.

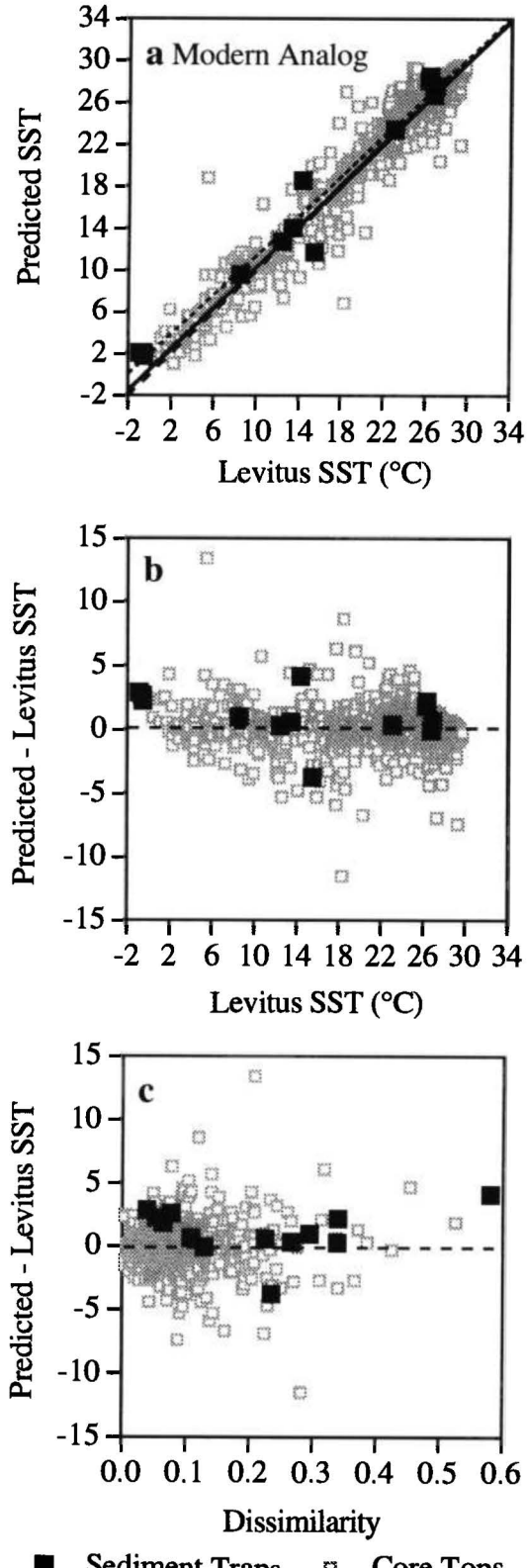

Figure 5. Results of the global modern analog method. Dashed and solid lines are as defined in Figure 4. (a) *Levitus* [1982] SST versus predicted SST. (b) Levitus SST versus residual SST. (c) Residual SST versus average sample dissimilarity. Greater dissimilarity denotes less similar samples.

Table 5. Global Imbrie-Kipp and Modern Analog Temperature Estimates for the Sediment Trap Faunas

Site	Average Dissimilarity	Sample Communality	Actual Temperature	Modern Analog Temperature	Modern Analog Residual	Imbrie-Kipp Temperature	Imbrie-Kipp Residual
Gulf of Alaska	0.34	0.16	8.5	9.5	1.0	12.9	4.4
Nearshore	0.34	0.70	12.4	12.7	0.3	13.8	1.4
Midway	0.22	0.63	13.4	14.0	0.6	16.2	2.7
Gyre	0.58	0.23	14.4	18.5	4.2	23.7	9.3
San Pedro Basin	0.23	0.61	15.5	11.7	-3.8	15.4	-0.1
Sargasso Sea	0.27	0.83	23.1	23.4	0.4	26.6	3.6
Central Pacific	0.34	0.39	26.3	28.5	2.2	29.5	3.1
Tropical Atlantic	0.13	0.94	26.8	26.7	-0.1	29.6	2.8
Panama Basin	0.11	0.97	26.9	27.5	0.6	24.6	-2.3
MANOP Site C	0.06	0.97	26.3	28.1	1.8	28.9	2.6
King George Basin	0.08	0.94	-0.6	2.0	2.6	2.9	3.5
North Weddell Sea	0.04	0.95	-0.9	2.0	2.9	3.3	4.2
Maud Rise	0.05	0.96	-0.5	1.7	2.2	3.4	3.9

Modern Analog Results

We assessed potential bias in the modern analog SST estimates in the same manner as with the Imbrie-Kipp transfer function. The modern analog SST estimates for the sediment trap samples are listed in Table 5. We determined modern analog SST for every sample in the core top database by comparing each sample against all other samples in the data set (Figure 5a). These core top MAT SST estimates have an RMS error of 1.5°C. The modern analog core top SST estimates have a slope of 0.98±0.01 and an intercept of 0.4±0.3 relative to *Levitus* [1982] SST.

When the core tops are used to estimate MAT SST values for each of the sediment trap faunas, the resulting estimates have an RMS error of 2.2°C and follow a slope of 0.95±0.15 and an intercept of 1.9±2.5 relative to *Levitus* [1982]. The modern analog method produced slopes and intercepts with no statistically significant difference between the core top and sediment trap data sets. The intercepts for the modern analog SST estimates were smaller than those for the global Imbrie-Kipp transfer function (Table 6). Unlike the result using the Imbrie-Kipp method, a two-sided *t*-test of the 1.2°C average MAT SST sediment trap residual demonstrates that this offset is not statistically different from zero (df=12, RMSE = 2.2°C, t-value=1.89 < t-crit@0.05=2.179). Using the core top data set, the slope for the modern analog method was closer to unity than the slope for the global Imbrie-Kipp transfer function. Modern analog SST residuals displayed no significant trends as a function of Levitus SST (Figure 5b) or average modern analog dissimilarity (Figure 5c). This was true for both the core top and sediment trap modern analog SST estimates.

Discussion

These two methods of estimating paleoceanographic temperature have received considerable scrutiny over the past two decades. However, not all of these studies have reached the same conclusions regarding the relative applicability of the two methods. *Prell* [1985] compared the two methods using core top and glacial maximum samples from the Atlantic, Indian, and Pacific basins. He concluded that they provided similar results within each basin and that transfer functions calibrated for a specific basin worked best in that basin. *Prell* [1985] did not present results for a global comparison, nor did his work include any modern sediment trap samples. *Anderson* et al. [1989] made downcore comparisons of the two methods in the Coral Sea and also concluded the two methods provided similar results. Their findings accentuated the discrepancies between marine SST estimates which suggest little cooling of the LGM low-latitude Pacific and terrestrial temperature estimates which imply a much larger low-latitude thermal decrease.

Working with a calibration data set composed of 499 Pacific

Table 6. Statistical Comparison of the Two Methods

	Core top Faunal Comparison (N=1121)				Sediment Trap Faunal Comparison (N=13)			
Analysis Type	Mean Residual	RMS Error	Slope	Intercept	Mean Residual	RMS Error	Slope	Intercept
Global Imbrie-Kipp Transfer function	0.0	1.9	0.93±0.02[a]	1.7±0.4[a]	3.0[b]	2.6	0.92±0.16	4.2±2.8[a]
Modern analog method Temperature estimate	0.0	1.5	0.98±0.01	0.4±0.3	1.2	2.2	0.95±0.15	1.9±2.5

[a]Significant difference from 1 for slopes and from zero for intercepts at $p < 0.05$.
[b]Significant difference from zero at $p << 0.01$.

core tops, *Le* [1992] compared these methods at two sites in the western Pacific. The primary conclusion of *Le* [1992] was that the Imbrie-Kipp method provided consistent, reliable SST estimates and that the modern analog method did not. Methodological differences between the study of *Le* [1992] and those of *Prell* [1985] and our study must be addressed. *Le* [1992] compared the two methods using 18 and 33 species for modern analog calculations and a subset of 24 species for transfer function calculations. This introduces a second variable into the comparison, making it difficult to determine if the obtained results are fundamental or potentially related to differences in the species lists. *Le* [1992] made use of a smaller calibration data set than *Prell* [1985] or this study and evaluated the methods by comparing downcore SST estimates from two cores in a relatively small, low-latitude region. The first of these factors decreases the range of hydrographic variation included in the calibration data set, while the second decreases the range of temperature variation over which the two methods were assessed. While evaluating the temporal response of the two methods provides indications of their precision, it cannot assess their accuracy at reconstructing true SST variation because of the lack of a priori knowledge of the true paleotemperatures. For these reasons, we employ global data sets of coretop and sediment trap faunas as a means of assessing both the accuracy and precision of the two methods over the observed global SST range.

Comparisons of Both Methods

To evaluate the temperature biases associated with the modern analog and global Imbrie-Kipp SST estimates, we calculated simple linear regressions of actual SST against estimated SST for both the coretop and sediment trap data sets (Figures 4 and 5). Four regression statistics (slope, intercept, RMS error, and mean residual value) are summarized in Table 6. A slope significantly different from 1 indicates residual trends in the SST estimates. A regression intercept or a mean residual value significantly different from zero indicates a constant offset in the SST estimates relative to the actual SST if the slope of the regression is not significantly different from unity. Larger RMS errors indicate greater random error in the SST estimates. Thus minimal temperature bias is displayed when slopes are close to 1, intercepts are close to zero, and RMS errors are small.

Temperature estimates derived from the coretop data set (N=1121) using the modern analog method came closest to this ideal, with a slope of 0.98±0.01, an intercept of 0.4±0.3, and an RMS error of 1.5°C (Table 6). The variability associated with the slope and intercept of the regression are within the 95% confidence interval of the statistic. Using the same core top data set but estimating SST with the global Imbrie-Kipp transfer function method resulted in greater temperature bias. This can be seen by comparing the coretop statistics down each column in Table 6. The statistics for the coretop global Imbrie-Kipp transfer function yield a slope of 0.93±0.02, which is significantly different from one, an intercept of 1.7±0.4, which is significantly different from zero, and an RMS error of 1.9°C, almost 0.5°C larger than the RMS error for the modern analog method (Table 6).

Temperature bias in the Imbrie-Kipp method for the sediment trap faunas was expressed as a slope of 0.92±0.16, a nonzero intercept of 4.2±2.8, and an RMS error of 2.6°C. The statistics for the modern analog method using the sediment trap data set were a slope of 0.95±0.15, an intercept of 1.9±2.5, and an RMS error of 2.2°C (Table 6). The confidence intervals associated with the much smaller sediment trap data set (N=13) are wider than those of the larger, coretop data set (N=1121). As a result, using the sediment traps, both methods produced SST estimates with slopes that were not significantly different from unity relative to observed SST (with 95% confidence). However, using the small sample two-sided t-test, we demonstrate that the mean residual value of the Imbrie-Kipp method was significantly different from zero (with 99% confidence), while the mean residual value produced by the modern analog method was not significantly different from zero. This was the same pattern observed for the regression intercepts with the much larger core top data set.

The greatest potential systematic bias we observed using either the core top or sediment trap data was related to the differences in the intercepts of the actual versus estimated SST regressions for the two methods. Using the core top data set, the Imbrie-Kipp method generated an intercept of 1.7±0.4°C relative to *Levitus* [1982] SST. This value is 1.3°C warmer than the 0.4°C±0.3 intercept of the modern analog method for the coretop data set (Table 6).

Because Imbrie-Kipp transfer functions are often developed for specific oceanic regions, we generated two additional factor models and Imbrie-Kipp transfer functions using (1) only samples from sites >8°C and (2) only samples from sites >20°C. The RMS error in the >8°C equation was 1.9°C, while that for the >20°C equation was 1.3°C. Despite RMS errors smaller or equal to the global Imbrie-Kipp equation, both regional equations had more significant, systematic temperature bias than the global relationship (Figure 6). This finding suggests the need for great caution when regional Imbrie-Kipp transfer functions are employed. Extreme SST errors can occur if a downcore foraminiferal fauna was generated when the true paleotemperature was outside the calibration range of the data set (i.e., during "no-analog" situations). Temperature estimates within the thermal bounds of the data set may also be questionable due to the systematic residual bias.

The results in Figure 5, Table 5, and Table 6 indicate that the modern analog method provides relatively unbiased estimates of SST over a range of almost 30°C. This result is particularly impressive when one considers the relatively poor quality of the core top analogs which were identified for many of the sediment trap assemblages. In 7 of the 13 cases, the average dissimilarity coefficient was >0.20, the critical threshold we discuss in the methods section. While we do not recommend relaxing this constraint in downcore studies, the robustness of the method is demonstrated by the fact that even when pushed well beyond the scope of its geologic application parameters, it still provided relatively accurate SST values for most of the sediment trap localities.

The two most severe SST errors in the sediment trap comparison occurred for traps in the San Pedro Basin (-3.8°C) and at the Multitracers Gyre site (+4.2°C). Both of these sites are located in the California Current region where coretops are relatively scarce and calcite dissolution is heavy. At least some of the temperature error associated with these two traps must arise from inadequacy of the coretop calibration data set. While both of the errors described above are serious, similar

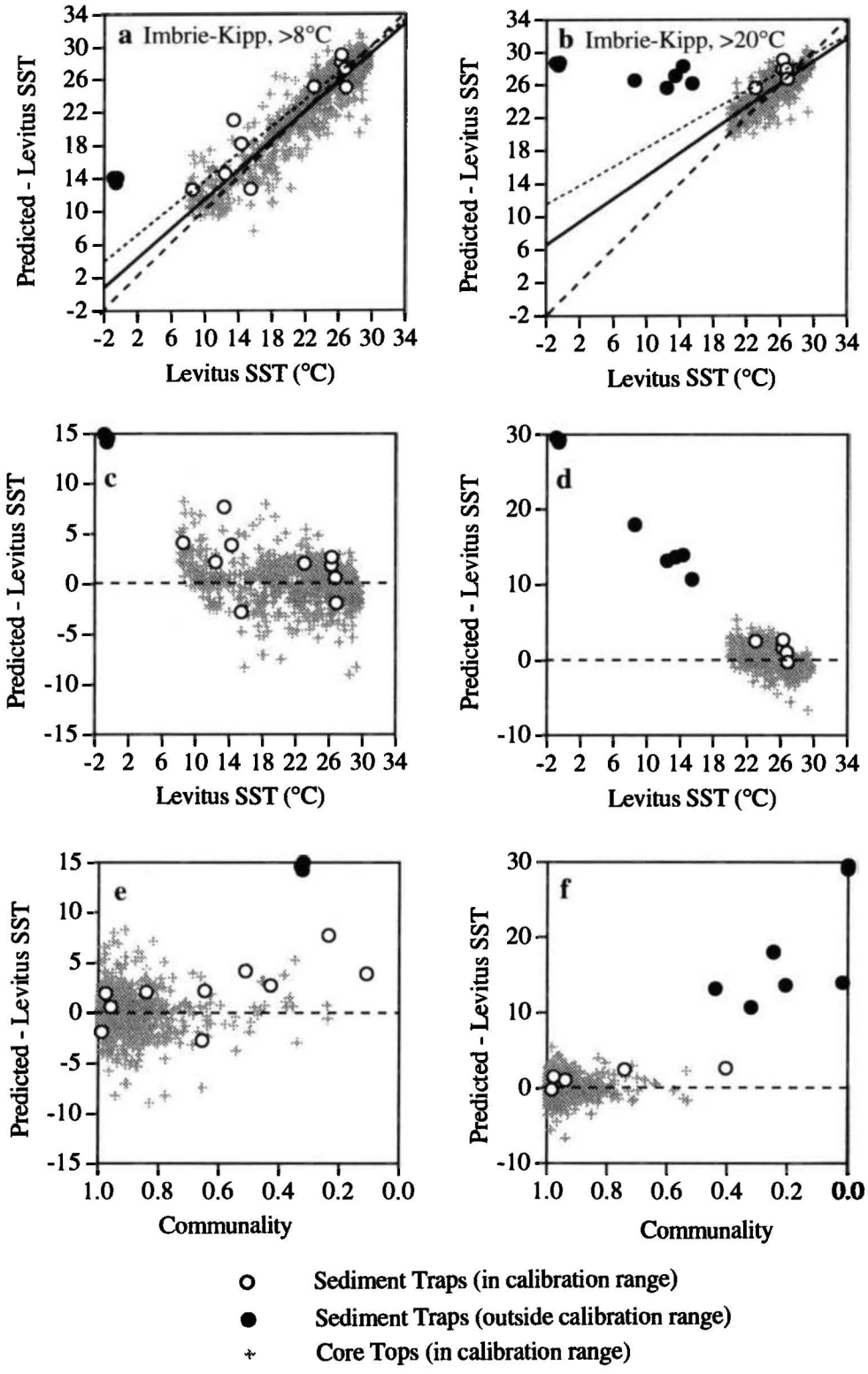

Figure 6. Results of the culled Imbrie-Kipp transfer functions. Dashed and solid lines are as defined in Figure 4. Figures 6a, 6c, and 6e show transfer function based on all core tops >8°C. Figures 6b, 6d, and 6f show transfer function based on all core tops >20°C. Note reversed communality axis.

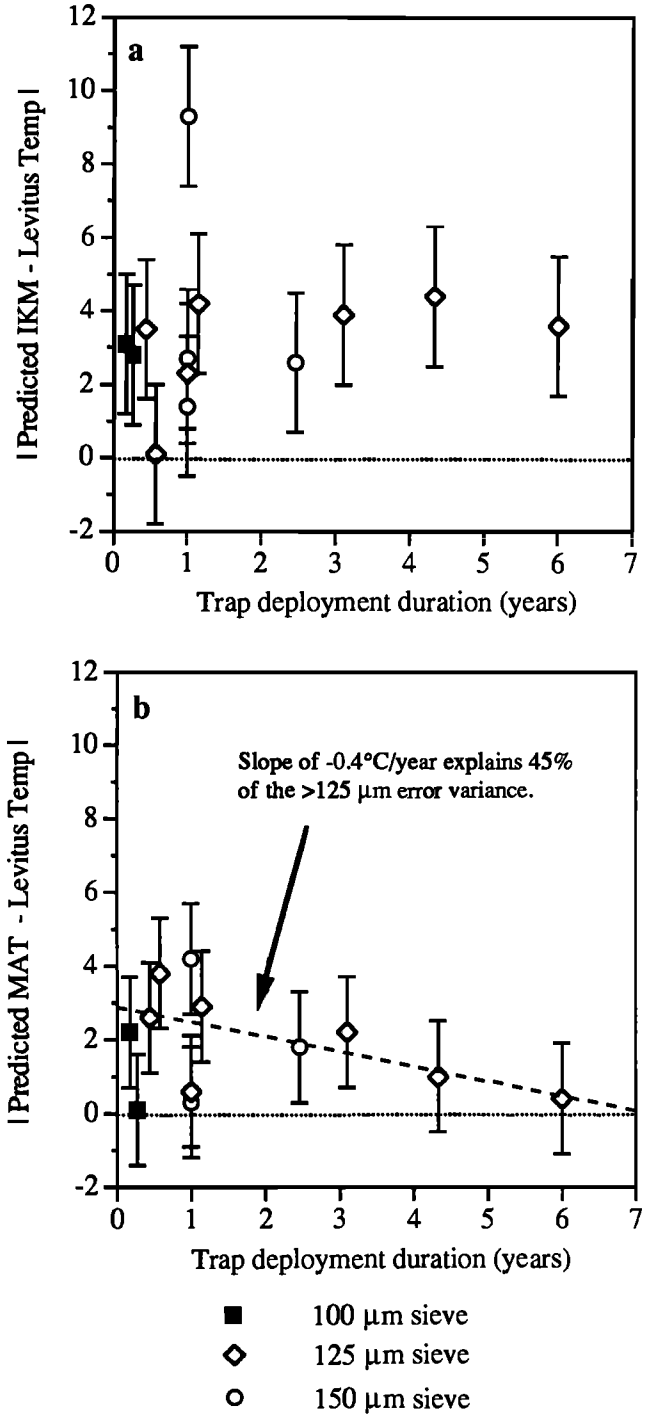

Figure 7. Absolute magnitude of the sediment trap SST residuals for (a) the Imbrie-Kipp method and (b) the modern analog method as a function of the sediment trap deployment duration and seive size. Slope in Figure 7b is based on a least squares regression of the >125 µm samples only.

situations are avoidable in downcore applications by careful attention to the quality of the modern analogs as indicated by the magnitude of the dissimilarity coefficient. In a sediment application, erroneous SST estimates such as those at Gyre and the San Pedro Basin would not be predicted if a critical dissimilarity threshold of 0.20 were used as a cutoff criteria.

Assessing Potential Bias in the Sediment Trap Data Set

We observed that the basic structure of the sediment trap and core top faunas relative to SST were comparable by applying the coretop factor model to the sediment trap data set. The greatest differences between the two data sets occurred in midlatitude faunas which had relatively poor communalities and large modern analog dissimilarities relative to coretops (Table 5). These differences between the two data sets may occur because (1) the global factor model does not adequately resolve foraminiferal faunal variability in the midlatitudes, (2) delicate, soluble individuals in the sediment trap faunas are unlikely to be well preserved in the geologic record, or (3) the difference between the sediment trap and coretop data set is due to sieving artifacts and/or the duration of trap deployment.

We will address the third point before dealing with the other two possibilities. If the difference between the two data sets were due to artifact alone, we predict that the absolute magnitude of the sediment trap residuals would increase as sieve size moved farther from the standard >150 µm sieve size and would decrease with increasing trap duration. Perhaps surprisingly, the absolute SST residuals from both the Imbrie-Kipp and modern analog methods do not indicate any systematic dependence on sieve size (Figure 7). Indeed the >100 µm sieved samples that were deployed for the shortest overall duration exhibit smaller error than most of the >125 µm and >150 µm sieved samples. One explanation for this curious result is that these samples were collected from sediment traps deployed in tropical regions where small species are relatively uncommon [e.g., *Bradshaw*, 1959]. A second example serves to illustrate this point further. Small species, particularly *G. quinqueloba*, are present in high relative abundance in the >125 µm integrated sediment trap samples from the Gulf of Alaska and the San Pedro basin. This accounts in large part for the low communality and high dissimilarities of these two integrated sediment trap samples (Table 5). While the extreme dissimilarity and low communality for the Gulf of Alaska sample might indicate its temperature estimate should be very poor, it actually produces a temperature estimate with less error than the San Pedro trap sample. The observation that coretops from the vicinity of the Gulf of Alaska core are somewhat more common than those from the San Pedro Basin in the coretop data set provides a plausible explanation. In short, sieve size does not appear to exhibit any systematic effects on the SST residuals in the sediment trap data set.

Three key points can be made with respect to sediment trap duration. First, the Imbrie-Kipp method produced residuals that were independent of sediment trap duration (Figure 7a). This result seems plausible, as the errors in the Imbrie-Kipp temperature regression are largely a function of the structure of the coretop faunas that determine the terms in the transfer function. Additionally, the use of factor analysis acts to filter the sediment trap observations of random variations. In contrast, modern analog SST residuals tend to decrease with longer trap deployments (Figure 7b). Again, such a trend seems plausible. Longer integration times should result in samples with increasing similarity to fossil faunas. The trend accounts for roughly 45% of the error variance in the seven >125 µm sieved samples. Interestingly, errors that are not statistically

different from zero are achieved by the two sediment trap faunas with deployment duration of 4-6 years.

This result casts doubt on the conventional wisdom that argues sediment traps are not directly comparable to core tops because of their differences in integration time (months to years in sediment traps versus decades to millennia in core tops). One way to explain this result is that variance at an annual cycle dominates living foraminiferal assemblages, while variance at interannual time scales is significantly smaller. If so, a few years of sediment trap deployment would capture the long-term mean assemblage with sufficient precision for calibration with temperature data collected over the last few decades, or for comparison with geologic samples that accumulated in the last few thousand years.

To summarize, sieve size does not appear to play a dominant factor in determining the magnitude of the SST errors recorded by these sediment trap faunas. Sediment trap duration does not appear to contribute significantly to the Imbrie-Kipp SST errors but could account for up to 45% of the variance in the modern analog temperature estimates. Sediment trap records of more than 4 years duration appear sufficient to provide average assemblages analogous to those in geologic samples. Because significant sources of error between the sediment trap and core top sediments remain, we explore the two remaining alternative hypotheses: (1) the global factor model does not adequately resolve foraminiferal faunal variability in the midlatitudes and (2) delicate, soluble individuals in the sediment trap faunas are unlikely to be well preserved in the geologic record.

The first possibility seems unlikely. For example, several of the factors exhibit high factor loadings in the midlatitude temperature range (Figure 3), suggesting model terms of significance to these regions have been isolated. Dismissing the first possibility leads us to conclude that the second possibility, dissolution, may play a role in the sediment trap versus core top differences. Although the results were considerably noisy, the sediments appear to be enriched in robust species which remain after the dissolution of more fragile species from the sediment trap faunas. Despite these differences, the coretop calibration data set estimated accurate SST for most of the sediment trap faunas. In the final section, we explore the error at Gyre in closer detail as a means of evaluating this potential dissolution bias in the sediment record.

Assessing Potential Dissolution Bias in the Core Top Data Set

The Gyre sediment trap is located in the California Current, 650 km off the southern Oregon coast. On a seasonal basis, this site shifts from a summer/fall subtropical fauna dominated by *O. universa* and *G. ruber* to a diverse winter/spring fauna rich in right-coiling *N. pachyderma*, *N. dutertrei*, *G. glutinata*, *G. quinqueloba*, *G. bulloides*, and *G. falconensis*. The remainder of the species in this fauna include *G. calida*, *T. humilis*, *and G. scitula* [*Ortiz and Mix*, 1992]. The resulting flux-weighted annual average fauna is composed of 37% *O. universa* and 13% *G. ruber*.

In the underlying core top sediments of the northeast Pacific, *O. universa* and *G. ruber* accounts for 0-5% of the foraminiferal assemblage [*Coulbourn* et al. 1980]. An annually averaged abundance of 37% for *O. universa* exceeds

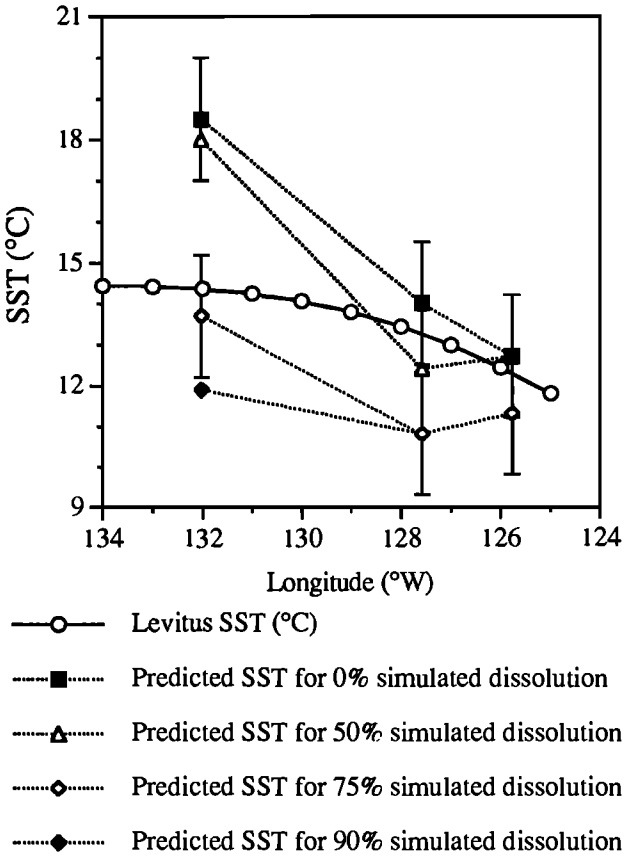

Figure 8. Effects of numerical dissolution scenarios on modern analog temperature estimates from the Multitracers sediment traps. Error bars of ±1.5°C apply in all cases but for clarity are shown only for 0% and 75% simulations. See text for further details.

expectations for its relative abundance in the underlying recent sediments by at least 32%. Moreover, the 37% abundance for *O. universa* exceeds the maximum abundance for this species recorded in the entire global coretop data base by 19%. The 13% abundance for *G. ruber* exceeds expectations for its relative abundance in the underlying sediments by at least 8%. Because these two species are indicative of warmer waters than the remainder of the species in the Gyre fauna, and both are relatively sensitive to dissolution, it seems likely they contribute heavily to the 4.2°C warm temperature bias at the Gyre site.

To evaluate the contribution of these two species to this problem, we recalculated modern analog SST for the three sediment traps in the Multitracers transect after "numerically dissolving" the sediment trap faunas (Figure 8). We accomplished this by making very simple assumptions of how dissolution might affect these samples. These assumptions are that *O. universa* and *G. ruber* would be removed at equal rates at all three sites and that no dissolution of other species would occur. This provides a very simple scenario for evaluating the impact of these two species on estimated SST while holding all other variables constant. Sensitivity studies were carried out on faunas with 50%, 75%, and 90% of the individuals of these

species removed from the faunal list. The various species percentages were recalculated following each "dissolution" step to preserve percent abundance closure, and then modern analog SST estimates were generated for the new fauna.

Removal of up to 50% of the individuals of these two species results in SST estimates which overlap within errors with the initial modern analog SST estimates for these three samples (Figure 8). Thus the modern analog method is quite robust to moderate dissolution. Removal of 75% of the individuals of these two species from the Gyre fauna resulted in SST estimates which were similar to the historically recorded SST at that site. In the more coastal sites, removing greater than 50% of these two species resulted in SST underestimates of 1°-3°C. This result suggests the Gyre site thermal bias derives from the high relative abundance of *O. universa* and *G. ruber* in the sediment traps at the Gyre site, a no-analog condition in the traps relative to the regional coretops due to the removal by dissolution of these fragile species from the fossil assemblage. Unfortunately, simply culling these species from the list used in the calculation of sample dissimilarities does not solve this preservation problem. We conducted additional experiments in which we excluded these two species from the taxonomic list and then recalculated modern analog SST. In the absence of these species from the dissimilarity function matrix, analogs for slightly more northern latitudes are selected, and the resulting modern analog SST underestimates the true SST.

Conclusions

We reassessed the utility of the Imbrie-Kipp and modern analog methods of estimating paleotemperature from foraminiferal faunas. Our approach differs from previous sediment based calibration studies because we use global core top faunas for calibration and sediment trap faunas for validation. Our results can be summarized as follows.

1. The basic structure of the sediment trap and coretop faunal assemblages are comparable. The greatest difference occurs in midlatitude faunas where the sediment traps have poor communalities relative to coretops. These differences may arise from the scarcity of coretops in midlatitude regions as well as the presence of delicate, soluble forms in the sediment traps which are unlikely to be well preserved in sediments. Despite these differences, the coretop calibration data set effectively estimated SST for most of the sediment trap faunas.

2. The modern analog method exhibited less systematic and random bias than the Imbrie-Kipp method over the full range of global SST.

3. Regional Imbrie-Kipp transfer functions exhibited greater systematic bias and equal or smaller random bias than the global Imbrie-Kipp transfer function we developed.

Acknowledgments. We thank the captain and crew of R/V *Wecoma* and the Multitracers sediment trap group for their efforts during the Multitracers sediment trap cruises. Early versions of the manuscript were improved by comments from N. Pisias, P. Wheeler, M. Abbott, and D. Birkes. We thank W. Prell, D. Andreasen, and two anonymous reviewers for their helpful reviews. Funding for this project was provided by a NASA Graduate student fellowship to the first author and by NSF funding to the Multitracers project. Curation of the Multitracers sediment trap samples at the NORCOR Marine Geological Repository at OSU was provided by a grant from the NSF. This is Lamont-Doherty Earth Observatory contribution 5598.

References

Anderson, D.M., W.L. Prell, and N.J. Barratt, Estimates of sea surface temperature in the coral sea at the last glacial maximum, *Paleoceanography*, *4*, 615-627, 1989.

Beck, J.W., R.L. Edwards, E. Ito, F.W. Taylor, J. Recy, F. Rougerie, P. Joannot, and C. Heinin, Sea-surface temperature from coral skeletal strontium/calcium ratios, *Science*, *257*, 644-647, 1992.

Bradshaw, J., Ecology of living planktonic foraminifera in the north and equatorial Pacific Oceans, *Contrib. Cushman Found., Foraminiferal Res.*, *10*, 25-64, 1959.

Broccoli, A.J., and E.P. Marciniak, Comparing simulated glacial climate and paleodata: A reexamination, *Paleoceanography*, *11*, 3-14, 1996.

Broecker, W.S., Oxygen isotope constraints on surface ocean temperatures, *Quat. Res.*, *26*, 121-134, 1986.

Climate: Long-Range Investigation, Prediction, and Mapping (CLIMAP) Project Members, The surface of the ice age Earth, *Science*, *191*, 1131-1137, 1976.

CLIMAP Project Members, Seasonal reconstructions of the earth's surface at the last glacial maximum, *Geol. Soc. Am. Map Chart Ser.*, *MC-36*, 1-18, 1981.

Coulbourn, W.T., F.L., Parker, and W.H. Berger, Faunal and solution patterns of planktonic foraminifera in surface sediments of the North Pacific, *Mar. Micropaleontol.*, *5*, 329-399, 1980.

Deuser, W.G., Seasonal variation in isotopic composition and deep-water fluxes of the tests of perennially abundant planktonic foraminifera of the Sargasso Sea: Results from sediment-trap collections and their paleoceanographic significance, *J. Foraminiferal Res.*, *17*, 14-27, 1987.

Deuser, W.G., and E.H. Ross, C., Seasonally abundant planktonic foraminifera of the Sargasso Sea: succession, deep-water fluxes, isotopic compositions, and paleoceanographic implications, *J. Foraminiferal Res.*, *19*, 268-293, 1989.

Donner, B., and G. Wefer, Flux and stable isotopic composition of *Neogloboquadrina pachyderma* and other planktonic foraminifers in the Southern Ocean (Atlantic sector), *Deep Sea Res., Part I*, *41*, 1733-1743, 1994.

Fairbanks R., and P.H. Wiebe, Foraminiferal and chlorophyll maximum: Vertical distribution, seasonal succession, and paleoceanographic significance, *Science*, *209*, 1524-1526, 1980.

Guilderson, T., R.G. Fairbanks, and J.L. Rubenstone, Tropical temperature variations since 20,000 years ago: Modulating interhemispheric climate change, *Science*, *263*, 663-665, 1994.

Hutson, W.H., The Agulhas Current during the Late Pleistocene: Analysis of modern faunal analogs, *Science*, *207*, 64-66, 1980.

Imbrie, J., and N.G. Kipp, A new micropaleontological method for quantitative paleoclimatology: Application to a Late Pleistocene Caribbean core, in *The Late Cenozoic Glacial Ages*, edited by K. Turekian, pp. 71-181, Yale Univ. Press, New Haven, Conn., 1971.

Kipp, N.G., New transfer function for estimating past seasurface conditions from sea level distribution of planktonic foraminifera in the North Atlantic, *Geol. Soc. Am. Mem.*,*v. 18*, 3-41, 1976.

Le, J., Palaeotemperature estimation methods: Sensitivity test on two western equatorial pacific cores, *Quaternary Science Reviews*, *11*, 801-820, 1992.

Levitus, S., Climatological atlas of the world ocean, *NOAA Prof. Pap. 13*, 173 pp. U.S. Govt. Print. Off., Washington, D.C. 1982.

Molfino, B., N.G. Kipp, and J. Morley, Comparison of foraminiferal, Coccolithophorid, and Radiolarian paleotemperature equations: Assemblage coherency and estimate concordancy, *Quat. Res.*, *17*, 279-313, 1982.

Ortiz, J.D., and A.C. Mix, The spatial distribution and seasonal succession of planktonic foraminifera in the California Current off Oregon, September 1987-1988, in *Upwelling Systems: Evolution Since the Early Miocene*, edited by C.P. Summerhayes, W.L. Prell, and K.C. Emeis, 197-213, *Geol. Soc. Spec. Publ.*, *64*, 1992.

Ortiz, J.D., A.C. Mix, and R.W. Collier, Environmental control of living symbiotic and asymbiotic planktonic foraminifera in the California Current, *Paleoceanography*, *10*, 987-1009, 1995.

Overpeck, J.T., T. Webb, and I.C. Prentice, Quantitative interpretation of fossil pollen spectra: Dissimilarity coefficients and the method of modern analogs, *Quat. Res., 23*, 87-108, 1985.

Parker, F.L., and W.L. Berger, Faunal and solution patterns of planktonic foraminifera in surface sediments of the South Pacific, *Deep Sea., 18*, 73-107, 1971.

Pflaumann, U., J. Duprat, C. Pujol, and L.D. Labeyrie, SINMAX: A modern analog technique to deduce Atlantic sea surface temperatures from planktonic foraminifera in deep-sea sediments, *Paleoceanography, 11*, 15-36, 1996.

Prell, W.L., The stability of low-latitude sea-surface temperatures: An evaluation of the CLIMAP reconstruction with emphasis on the positive SST anomalies, Rep. TR025, 60 P., U.S. Dep. of Energy, Washington DC, 1985.

Prentice, I.C., Multidimensional scaling as a research tool in Quaternary palynology: A review of theory and methods, *Rev. Paleobot. and Palynol., 31*, 71-104, 1980.

Rind, D., and D. Peteet, Terrestrial conditions at the Last Glacial Maximum and CLIMAP sea-surface temperature estimates: Are they consistent?, *Quat. Res., 24*, 1-22, 1985.

Sauter, L., and R. Thunell, Seasonal succession of the planktonic foraminifera: Results from a four year time-series sediment trap experiment in the northern Pacific, *J. Foraminiferal Res., 19*, 253-267, 1989.

Sauter, L, and Thunel, Planktonic foraminiferal response to upwelling and seasonal hydrographic conditions: Sediment trap results from San Pedro basin, southern California, *J. Foraminiferal Res., 21*, 347-363, 1991.

Stott, L., and C.M. Tang, Reassessment of foraminiferal-based tropical sea surface $\delta^{18}O$ paleotemperatures, *Paleooceanog., 11*, 37-56, 1996.

Thompson, P.R., Planktonic foraminifera in the western North Pacific during the past 150,000 years: Comparison of modern and fossil assemblages, *Palaeogeogr. Palaeoclimator. Palaeoecol., 35*, 241-279, 1981

Thunnell, R.C., and S. Honjo, Planktonic foraminiferal flux to the deep ocean: Sediment trap results from the Tropical Atlantic and the Central Pacific, *Mar. Geo., 40*, 237-253, 1981.

Thunnell, R.C., and L.A. Reynolds, Sedimentation of planktonic foraminifera: Seasonal changes in species flux in the panama Basin, *Micropaleo., 30*, 243-262, 1984.

Watkins, J., A.C. Mix, and J. Wilson, Living planktonic foraminifera: Tracers of circulation and productivity regimes in the central equatorial pacific, *Deep Sea Res., Part II*, in press, 1996.

A.C. Mix, College of Oceanic and Atmospheric Sciences, Oregon State University, Corvallis, OR 97331-5503. (email: amix@oce.orsat.edu)
J.D. Ortiz, Lamont-Doherty Earth Observatory of Columbia University, Palisades, NY 10964. (email: jortiz@ldeo.columbia.edu)

(Received November 29, 1995; revised September 16, 1996; accepted September 23, 1996.)